



CERN-EP-2018-172
 LHCb-PAPER-2018-026
 October 18, 2018

First observation of the doubly charmed baryon decay

$$\Xi_{cc}^{++} \rightarrow \Xi_c^+ \pi^+$$

LHCb collaboration[†]

Abstract

The doubly charmed baryon decay $\Xi_{cc}^{++} \rightarrow \Xi_c^+ \pi^+$ is observed for the first time, with a statistical significance of 5.9σ , confirming a recent observation of the baryon in the $\Lambda_c^+ K^- \pi^+ \pi^+$ final state. The data sample used corresponds to an integrated luminosity of 1.7 fb^{-1} , collected by the LHCb experiment in pp collisions at a center-of-mass energy of 13 TeV . The Ξ_{cc}^{++} mass is measured to be

$$3620.6 \pm 1.5 \text{ (stat)} \pm 0.4 \text{ (syst)} \pm 0.3 \text{ (}\Xi_c^+\text{) MeV}/c^2,$$

and is consistent with the previous result. The ratio of branching fractions between the decay modes is measured to be

$$\frac{\mathcal{B}(\Xi_{cc}^{++} \rightarrow \Xi_c^+ \pi^+) \times \mathcal{B}(\Xi_c^+ \rightarrow p K^- \pi^+)}{\mathcal{B}(\Xi_{cc}^{++} \rightarrow \Lambda_c^+ K^- \pi^+ \pi^+) \times \mathcal{B}(\Lambda_c^+ \rightarrow p K^- \pi^+)} = 0.035 \pm 0.009 \text{ (stat)} \pm 0.003 \text{ (syst)}.$$

Published in Phys. Rev. Lett. **121**, 162002 (2018)

© 2018 CERN for the benefit of the LHCb collaboration. CC-BY-4.0 licence.

[†]Authors are listed at the end of this paper.

The recent observation by the LHCb collaboration [1] of a new state that is consistent with the doubly charmed baryon Ξ_{cc}^{++} , opens a new field of research studying the properties of baryons containing two heavy quarks, providing a unique environment for testing models of quantum chromodynamics (QCD). In studies of a sample of Ξ_{cc}^{++} decays to the final state $\Lambda_c^+ K^- \pi^+ \pi^+$, with $\Lambda_c^+ \rightarrow p K^- \pi^+$, its mass was found to be 3621.40 ± 0.72 (stat) ± 0.27 (syst) ± 0.14 (Λ_c^+) MeV/ c^2 [1], and its lifetime was measured to be $0.256^{+0.024}_{-0.022}$ (stat) ± 0.014 (syst) ps [2].¹ The measured lifetime firmly establishes its weakly decaying nature. Searching for new decay modes is the next critical step towards understanding the dynamics of weak decays of doubly heavy baryons, which may differ significantly from those of singly heavy hadrons due to interference between decay amplitudes of the two heavy quarks. The process $\Xi_{cc}^{++} \rightarrow \Xi_c^+ \pi^+$ has been predicted to have a sizable branching fraction [3, 4], making it a promising final state in which to seek confirmation of the previous observation.

This Letter reports the first observation of the decay $\Xi_{cc}^{++} \rightarrow \Xi_c^+ \pi^+$, which proceeds predominantly via the tree-level amplitude represented by the Feynman diagram shown in Fig. 1. The Ξ_c^+ baryon is reconstructed in its Cabibbo-suppressed decay to $p K^- \pi^+$. The data sample used consists of pp collisions at a center-of-mass energy of 13 TeV collected by the LHCb experiment in 2016, corresponding to an integrated luminosity of 1.7 fb^{-1} . A measurement of the Ξ_{cc}^{++} mass with this sample is presented, and the ratio of the total branching fractions, $\mathcal{R}(\mathcal{B})$, between the decays $\Xi_{cc}^{++} \rightarrow \Xi_c^+ (\rightarrow p K^- \pi^+) \pi^+$ and $\Xi_{cc}^{++} \rightarrow \Lambda_c^+ (\rightarrow p K^- \pi^+) K^- \pi^+ \pi^+$ is determined.

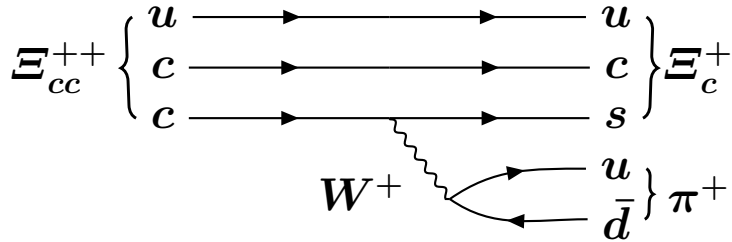


Figure 1: Dominant Feynman diagram contributing to the decay $\Xi_{cc}^{++} \rightarrow \Xi_c^+ \pi^+$.

The LHCb detector [5, 6] is a single-arm forward spectrometer covering the pseudorapidity range $2 < \eta < 5$, designed for the study of particles containing b or c quarks. The detector includes a high-precision tracking system consisting of a silicon-strip vertex detector [7] surrounding the pp interaction region that allows c and b hadrons to be identified from their typical long flight distance; a tracking system [8] that provides a measurement of momentum, p , of charged particles; two ring-imaging Cherenkov detectors [9] that discriminate between different species of charged hadrons; a calorimeter system consisting of scintillating-pad and preshower detectors, an electromagnetic calorimeter and a hadronic calorimeter, to identify photons, electrons and hadrons; a muon system composed of alternating layers of iron and multiwire proportional chambers [10] to identify muons. The online event selection is performed by a trigger [11], which consists of a hardware stage, based on information from the calorimeter and muon systems [12], followed by a

¹ The inclusion of charge-conjugate processes is implied throughout.

software stage, which applies a full event reconstruction incorporating real-time alignment and calibration of the detector [13]. The same alignment and calibration information is propagated to the offline reconstruction, ensuring consistent and high-quality particle identification (PID) information between the trigger and offline software. The identical performance of the online and offline reconstruction offers the opportunity to perform physics analyses directly using candidates reconstructed in the trigger which is done in the present analysis.

Simulation is required to model the effects of the detector acceptance and the imposed selection requirements. In the simulation, pp collisions are generated using PYTHIA [14] with a specific LHCb configuration [15]. A dedicated generator, GENXICC2.0 [16], is used to simulate Ξ_{cc}^{++} baryon production. Decays of hadrons are described by EVTGEN [17], in which final-state radiation is generated using PHOTOS [18]. The interaction of the generated particles with the detector, and its response, are modelled using the GEANT4 toolkit [19] as described in Ref. [20].

The selection of $\Xi_{cc}^{++} \rightarrow \Xi_c^+ (\rightarrow pK^-\pi^+)\pi^+$ decays is designed to be as similar as possible to those of $\Xi_{cc}^{++} \rightarrow \Lambda_c^+ (\rightarrow pK^-\pi^+)K^-\pi^+\pi^+$, described in Ref. [1]. Three charged particles identified as p , K^- and π^+ that form a good-quality vertex are combined to reconstruct a $\Xi_c^+ \rightarrow pK^-\pi^+$ candidate. The three particles are required to have transverse momenta in excess of $500\text{ MeV}/c$ and be inconsistent with originating from any primary vertex (PV). The Ξ_c^+ vertex is required to be displaced from any PV by a distance corresponding to a Ξ_c^+ decay time greater than 0.15 ps , which corresponds to approximately twice the decay time resolution. The invariant-mass of each Ξ_c^+ candidate is required to be in the range $2450\text{--}2488\text{ MeV}/c^2$, corresponding to approximately six times the Ξ_c^+ mass resolution. An additional positively charged particle, which must be identified as a pion and have p_T greater than $200\text{ MeV}/c$, is then combined with the Ξ_c^+ candidate to form a Ξ_{cc}^{++} candidate. The $\Xi_c^+\pi^+$ pair is required to form a vertex that is of good quality and is upstream of the Ξ_c^+ vertex. The Ξ_{cc}^{++} candidate must have $p_T > 2000\text{ MeV}/c$ and be consistent with originating from a PV. The candidate is associated with the PV with respect to which it has the smallest impact parameter χ^2 (χ_{IP}^2). The χ_{IP}^2 is defined as the difference in χ^2 of the PV fit with and without the particle in question. To avoid contributions due to duplicate tracks, candidates are rejected if the angle between any pair of their final-state particles with the same charge is smaller than 0.5 mrad . Specific hardware trigger requirements are also applied, to increase the signal yield and simplify the study of the trigger efficiency. Candidates are retained only if the event contains large transverse energy deposits in the calorimeter arising from the decay products of the Ξ_{cc}^{++} candidate, or if the event contains activity either in the calorimeter or in the muon system from particles other than these decay products. Simulation shows that the efficiency for these additional requirements is above 90% for both two-body or four-body Ξ_{cc}^{++} decay modes.

A multivariate selector based on the multilayer perceptron algorithm [21] is used to further suppress combinatorial backgrounds. To train the selector, simulated $\Xi_{cc}^{++} \rightarrow \Xi_c^+ (\rightarrow pK^-\pi^+)\pi^+$ decays are used as a signal sample, and 0.3 million candidates from the upper sideband with invariant-masses in the range $3800\text{--}4000\text{ MeV}/c^2$ are used as a background sample. To reduce the effect of the Ξ_c^+ mass resolution on the invariant-mass of the Ξ_{cc}^{++} candidates, an alternative evaluation of the invariant-mass is used, $m(\Xi_c^+\pi^+) \equiv M(\Xi_c^+\pi^+) - M([pK^-\pi^+]_{\Xi_c^+}) + M_{\text{PDG}}(\Xi_c^+)$, where $M(\Xi_c^+\pi^+)$ and $M([pK^-\pi^+]_{\Xi_c^+})$ are the reconstructed masses of the Ξ_{cc}^{++} and Ξ_c^+ candidates, and

$M_{\text{PDG}}(\Xi_c^+)$ is the known value of the Ξ_c^+ mass [22].

The input variables used in the multivariate selector are chosen based on their discrimination power between signal and background candidates. Three different types of variables are considered in the training. The first type of variables are the kinematic information of particles, including the p_T of each of the four final-state particles and of the Ξ_c^+ and Ξ_{cc}^{++} candidates; the angle between the Ξ_{cc}^{++} momentum vector and the displacement vector from the PV to the Ξ_{cc}^{++} decay vertex. The second type of variables are the vertex fitting qualities, including the χ^2 per degree of freedom of the Ξ_c^+ and Ξ_{cc}^{++} vertex fits; the χ^2 per degree of freedom of a kinematic refit [23] of the $\Xi_{cc}^{++} \rightarrow \Xi_c^+(\rightarrow pK^-\pi^+)\pi^+$ decay chain that requires the Ξ_{cc}^{++} to originate from its PV. The third type of variables are related to the lifetime, including the χ^2_{IP} of each of the four final-state particles and of the Ξ_c^+ and Ξ_{cc}^{++} candidates with respect to their associated PV; the sum of the χ^2_{IP} of the four final-state particles; and the flight distance χ^2 of the Ξ_c^+ and Ξ_{cc}^{++} candidates. The flight distance χ^2 is defined as the χ^2 of the hypothesis that the decay vertex of the candidate coincides with its associated PV.

Candidates are retained only if the multivariate-selector output exceeds a certain threshold. This threshold is chosen to maximize the expected value of the figure of merit $\varepsilon/(5/2 + \sqrt{N_B})$ [24]. Here, ε is the estimated signal efficiency and N_B is the expected number of background candidates under the signal peak in the Ξ_{cc}^{++} mass distribution, after the selection. The quantity N_B is determined, assuming an exponential shape for the background, from the number of $\Xi_c^+\pi^+$ candidates in the mass region of 3800–4000 MeV/ c^2 , scaled to a signal region centered at a mass of 3620 MeV/ c^2 and with a width of 30 MeV/ c^2 . This corresponds to approximately five times the expected Ξ_{cc}^{++} mass resolution. To test for potential biases in the multivariate selection or other misreconstruction effects, the same selection criteria are applied to control samples of data consisting of $\Xi_c^+\pi^+$ candidates in the Ξ_c^+ sideband regions and of wrong-sign combination $\Xi_c^+\pi^-$. No peaking structure is visible in either samples.

Figure 2 (left) shows the distribution of invariant-masses of Ξ_{cc}^{++} candidates, $m(\Xi_c^+\pi^+)$, after applying the complete selection. The contribution from events containing multiple signal candidates is found to be less than 1%; all these candidates are included in the fit. A signal is visible at a mass of approximately 3620 MeV/ c^2 , in the vicinity of the previous LHCb Ξ_{cc}^{++} baryon observation [1]. The mass distribution is fitted with an unbinned extended maximum-likelihood method to measure the properties of this structure. The peak is described by an empirical model, consisting of a Gaussian function and a modified Gaussian function with power-law tails on both sides [25] and with the same mean value. All tail parameters are fixed to values obtained from a fit to simulated signal events, while the parameters corresponding to the mass and the mass resolution are varied in the fit. The background shape is described by an exponential function. The resulting signal yield is 91 ± 20 and the mass value is 3620.7 ± 1.5 MeV/ c^2 , where the uncertainties are statistical only. The mass is fully consistent with the value measured in the $\Xi_{cc}^{++} \rightarrow \Lambda_c^+ K^-\pi^+\pi^+$ decay channel [1], and the resolution determined by the fit is consistent with expectations based on known detector performance. The local statistical significance of the signal, evaluated by taking the likelihood ratio corresponding to fits that include and exclude the signal component, is found to be 5.9σ , thus confirming the observation reported in Ref [1].

The invariant-mass distribution for the reference mode, $\Xi_{cc}^{++} \rightarrow \Lambda_c^+ K^-\pi^+\pi^+$, is shown in Fig. 2 (right). The selection used to obtain this sample is identical to that of the previous analysis [1], except for the additional requirements on the hardware trigger. An

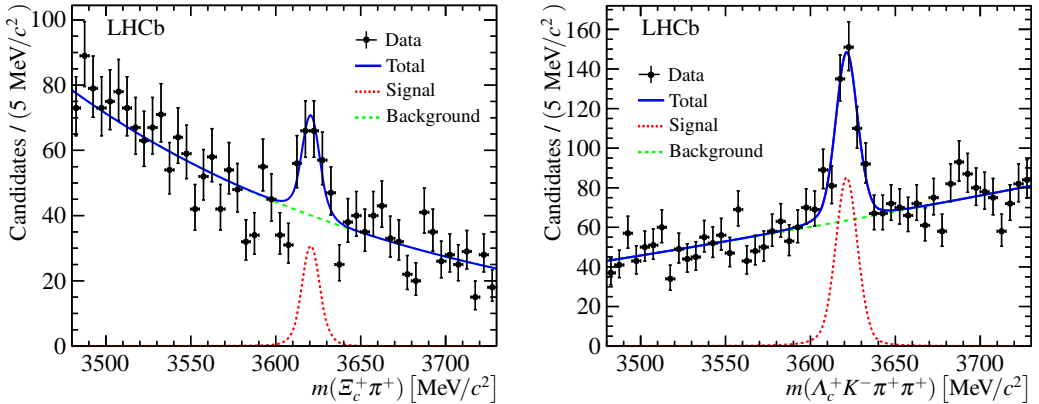


Figure 2: Invariant-mass distribution of the $\Xi_{cc}^{++} \rightarrow \Xi_c^+ \pi^+$ (left) and $\Xi_{cc}^{++} \rightarrow \Lambda_c^+ K^- \pi^+ \pi^+$ (right) candidates with result of the fit overlaid. The black points represent the data, the dotted (red) line represents the signal contribution, and the dashed (green) line represents the combinational background.

extended unbinned maximum-likelihood fit to the invariant-mass distribution returns a signal yield of 289 ± 35 for the reference mode.

The branching fraction ratio, $\mathcal{R}(\mathcal{B})$, between the decays $\Xi_{cc}^{++} \rightarrow \Xi_c^+ (\rightarrow pK^-\pi^+)\pi^+$ and $\Xi_{cc}^{++} \rightarrow \Lambda_c^+ (\rightarrow pK^-\pi^+)K^-\pi^+\pi^+$ is defined as

$$\mathcal{R}(\mathcal{B}) \equiv \frac{\mathcal{B}(\Xi_{cc}^{++} \rightarrow \Xi_c^+ \pi^+) \times \mathcal{B}(\Xi_c^+ \rightarrow pK^-\pi^+)}{\mathcal{B}(\Xi_{cc}^{++} \rightarrow \Lambda_c^+ K^-\pi^+\pi^+) \times \mathcal{B}(\Lambda_c^+ \rightarrow pK^-\pi^+)} = \frac{r_N}{r_\varepsilon}, \quad (1)$$

where r_N is the ratio of Ξ_{cc}^{++} yields between the signal and reference decay modes, and r_ε is the ratio of total efficiencies between the two modes. In each case, the total efficiency includes the effects of the geometrical acceptance, trigger, reconstruction, and selection. Each contribution to the efficiency ratio is evaluated with simulation, calibrated with data when possible, as described in the following. The combined efficiency of the reconstruction and the selection, excluding the hardware-trigger requirement, is determined from fully simulated signal samples in which the tracking [26] and particle-identification efficiencies are corrected using control samples. The correction to the efficiency ratio of the $\Xi_{cc}^{++} \rightarrow \Lambda_c^+ K^-\pi^+\pi^+$ and $\Xi_{cc}^{++} \rightarrow \Xi_c^+ \pi^+$ channels is determined to be 0.983 ± 0.007 for the tracking efficiency, and 1.050 ± 0.020 for the particle-identification efficiency. The hardware-trigger efficiency ratio is estimated from fully simulated signal events, with a p_T -dependent correction derived from data using $\Lambda_b^0 \rightarrow \Lambda_c^+ (\rightarrow pK^-\pi^+)\pi^-\pi^+\pi^-$ and $\Lambda_b^0 \rightarrow \Lambda_c^+ (\rightarrow pK^-\pi^+)\pi^-$ decays, which are required to pass the same trigger selection as the Ξ_{cc}^{++} candidates. These two decay channels have similar final states and decay topologies as the signal. The total relative efficiency is determined to be $r_\varepsilon = 0.110 \pm 0.002$, where the uncertainty comes from the limited size of the simulation sample and is accounted as a systematic uncertainty. To validate this procedure, the ratio of branching fractions of the decays $\Lambda_b^0 \rightarrow \Lambda_c^+ (\rightarrow pK^-\pi^+)\pi^-$ and $\Lambda_b^0 \rightarrow \Lambda_c^+ (\rightarrow pK^-\pi^+)\pi^-\pi^+\pi^-$ is measured using the same data sample, resulting in a value 0.83 ± 0.05 (statistical uncertainty only) which agrees with the previous LHCb result of 0.70 ± 0.10 [27].

The main sources of systematic uncertainty that affect the measurements of the

Ξ_{cc}^{++} mass are summarized in Table 1. Samples of $J/\psi \rightarrow \mu^+ \mu^-$ and $B^+ \rightarrow J/\psi K^+$ decays [28, 29] are used to calibrate the reconstructed momentum of charged particles, which affect the reconstructed mass of signal. The maximum difference between the correction factors determined with above-mentioned decays is found to be 0.03%, which corresponds to a systematic uncertainty of $0.38 \text{ MeV}/c^2$ on the measured Ξ_{cc}^{++} mass. The signal selection efficiency increases with the Ξ_{cc}^{++} decay time; combined with a correlation between the reconstructed mass and the reconstructed decay time, this induces a positive bias on the masses of both Ξ_{cc}^{++} and Ξ_c^+ candidates. The effect is studied with simulation and the bias on the measured Ξ_{cc}^{++} mass is found to be $+0.10 \pm 0.10 \text{ MeV}/c^2$, where the uncertainty is due to the limited size of the simulated samples. A correction to the Ξ_{cc}^{++} mass of $-0.10 \text{ MeV}/c^2$ is therefore applied, and a systematic uncertainty of $0.10 \text{ MeV}/c^2$ assigned. The dependence of this bias on the Ξ_{cc}^{++} lifetime is studied by weighting simulated events to different lifetime hypotheses; the change is found to be negligible for the measured Ξ_{cc}^{++} lifetime [2]. The description of the final-state radiation in simulation [18] can also cause a bias in the measured mass, which is estimated with pseudoexperiments. The correction is determined to be $+0.03 \text{ MeV}/c^2$, with a negligible uncertainty. The impact of the model used to fit the invariant-mass distribution on the measured mass is estimated by varying the shape parameters that are fixed according to simulation, using alternative signal and background models, and performing the fits over different mass ranges. The largest variation in the fitted Ξ_{cc}^{++} masses, $0.05 \text{ MeV}/c^2$, is taken as a systematic uncertainty. The current known value for the Ξ_c^+ mass [22] is used to compute the invariant-mass $m(\Xi_c^+ \pi^+)$ of the Ξ_{cc}^{++} candidate. Its uncertainty, $0.30 \text{ MeV}/c^2$, is assigned as a systematic uncertainty on the Ξ_{cc}^{++} mass.

The systematic uncertainties on the ratio $\mathcal{R}(\mathcal{B})$ are listed in Table 1 and are described as follows. The alternative fit models mentioned above result in different values of the ratio r_N . The largest relative deviation measured, 5.2%, is assigned as a systematic uncertainty on $\mathcal{R}(\mathcal{B})$. The relative efficiency of the tracking, particle identification and trigger are estimated using control samples, whose statistical uncertainties are taken as a systematic uncertainty on $\mathcal{R}(\mathcal{B})$. An additional uncertainty of 4.1% is assigned on the track-reconstruction efficiency due to uncertainties on the material budget of the detector and the modelling of hadronic interaction with the detector material. The particle-identification efficiency is determined in bins of particle momentum and pseudorapidity using control samples. The size of the bins is increased or decreased by a factor of two and the largest deviation on $\mathcal{R}(\mathcal{B})$ is assigned as systematic uncertainty related to the binning. An additional uncertainty of 4.2% on the hardware trigger efficiency is determined from the Λ_b^0 control samples described above, including a statistical uncertainty from the limited sample size, and an uncertainty that is determined by testing the procedure in simulation and taking the deviation as a systematic uncertainty. Combining the systematic uncertainties on the efficiency mentioned above, a systematic uncertainty of 6.5% on $\mathcal{R}(\mathcal{B})$ is assigned. Uncertainties from the Ξ_{cc}^{++} mass, lifetime and production spectra are investigated, and 1.2% is assigned as a systematic uncertainty. Different requirements on the Ξ_{cc}^{++} p_T are applied to select the $\Xi_{cc}^{++} \rightarrow \Xi_c^+ \pi^+$ and $\Xi_{cc}^{++} \rightarrow \Lambda_c^+ K^- \pi^+ \pi^+$ decays, and this may cause a bias if the p_T distribution of simulated Ξ_{cc}^{++} differs from that in data. To assess the size of this effect, the measurement is repeated applying the same p_T requirement to both modes. The difference in $\mathcal{R}(\mathcal{B})$ is found to be 0.7%. A separate measurement carried out with a cut-based selection gives a consistent result.

The value of $\mathcal{R}(\mathcal{B})$ is measured to be $0.035 \pm 0.009 \text{ (stat)} \pm 0.003 \text{ (syst)}$ and the

Table 1: Systematic uncertainties on the measurement of the Ξ_{cc}^{++} mass and of the ratio of branching fractions $\mathcal{R}(\mathcal{B})$ between the $\Xi_{cc}^{++} \rightarrow \Xi_c^+ \pi^+$ and the $\Xi_{cc}^{++} \rightarrow \Lambda_c^+ K^- \pi^+ \pi^+$ decay modes.

Source	Mass [MeV/ c^2]	$\mathcal{R}(\mathcal{B}) [\%]$
Momentum calibration	0.38	—
Selection bias correction	0.10	—
Fit model	0.05	5.2
Relative efficiency	—	6.5
Simulation modelling	—	1.2
Selection	—	0.7
Sum in quadrature	0.40	8.5

Ξ_{cc}^{++} mass is measured to be 3620.6 ± 1.5 (stat) ± 0.4 (syst) ± 0.3 (Ξ_c^+) MeV/ c^2 , which is consistent with the mass measured in the final state $\Lambda_c^+ K^- \pi^+ \pi^+$, 3621.40 ± 0.72 (stat) ± 0.27 (syst) ± 0.14 (Λ_c^+) MeV/ c^2 [1]. Averaging over the two measurements, the Ξ_{cc}^{++} mass is determined to be 3621.24 ± 0.65 (stat) ± 0.31 (syst) MeV/ c^2 (see the Appendix 1 for the comparisons between the measured Ξ_{cc}^{++} masses and combined result). The combination is performed using the Best Linear Unbiased Estimate (BLUE) method [30, 31]. In the combination, the systematic uncertainties are assumed to be uncorrelated except for the momentum scale calibration.

In summary, a new decay mode of the doubly charmed baryon $\Xi_{cc}^{++} \rightarrow \Xi_c^+ \pi^+$ is observed with a statistical significance of 5.9σ in a data sample of pp collisions collected by the LHCb experiment at a center-of-mass energy of $\sqrt{s} = 13$ TeV. The Ξ_{cc}^{++} mass is consistent with the previous LHCb result [1] and with most theoretical calculations of the Ξ_{cc}^{++} mass (see *e.g.* Ref. [32]). The ratio of the total branching fractions between this decay ($\Xi_{cc}^{++} \rightarrow \Xi_c^+ \pi^+$) and the reference mode ($\Xi_{cc}^{++} \rightarrow \Lambda_c^+ K^- \pi^+ \pi^+$) is consistent with the prediction of Ref. [4], which, however, has large uncertainties. Therefore, this measurement provides important information towards an improved understanding of the decays of doubly charmed baryons.

Acknowledgements

We thank Chao-Hsi Chang, Cai-Dian Lü, Wei Wang, Xing-Gang Wu, and Fu-Sheng Yu for frequent and interesting discussions on the production and decays of double-heavy-flavor baryons. We express our gratitude to our colleagues in the CERN accelerator departments for the excellent performance of the LHC. We thank the technical and administrative staff at the LHCb institutes. We acknowledge support from CERN and from the national agencies: CAPES, CNPq, FAPERJ and FINEP (Brazil); MOST and NSFC (China); CNRS/IN2P3 (France); BMBF, DFG and MPG (Germany); INFN (Italy); NWO (Netherlands); MNiSW and NCN (Poland); MEN/IFA (Romania); MinES and FASO (Russia); MinECo (Spain); SNSF and SER (Switzerland); NASU (Ukraine); STFC (United Kingdom); NSF (USA). We acknowledge the computing resources that are provided by CERN, IN2P3 (France), KIT and DESY (Germany), INFN (Italy), SURF (Netherlands), PIC (Spain), GridPP (United Kingdom), RRCKI and Yandex LLC (Russia), CSCS (Switzerland), IFIN-HH

(Romania), CBPF (Brazil), PL-GRID (Poland) and OSC (USA). We are indebted to the communities behind the multiple open-source software packages on which we depend. Individual groups or members have received support from AvH Foundation (Germany); EPLANET, Marie Skłodowska-Curie Actions and ERC (European Union); ANR, Labex P2IO and OCEVU, and Région Auvergne-Rhône-Alpes (France); Key Research Program of Frontier Sciences of CAS, CAS PIFI, and the Thousand Talents Program (China); RFBR, RSF and Yandex LLC (Russia); GVA, XuntaGal and GENCAT (Spain); Herchel Smith Fund, the Royal Society, the English-Speaking Union and the Leverhulme Trust (United Kingdom); Laboratory Directed Research and Development program of LANL (USA).

References

- [1] LHCb collaboration, R. Aaij *et al.*, *Observation of the doubly charmed baryon Ξ_{cc}^{++}* , Phys. Rev. Lett. **119** (2017) 112001, [arXiv:1707.01621](#).
- [2] LHCb collaboration, R. Aaij *et al.*, *Measurement of the lifetime of the doubly charmed baryon Ξ_{cc}^{++}* , Phys. Rev. Lett. **121** (2018) 052002, [arXiv:1806.02744](#).
- [3] N. Sharma and R. Dhir, *Estimates of W-exchange contributions to Ξ_{cc} decays*, Phys. Rev. **D96** (2017) 113006, [arXiv:1709.08217](#).
- [4] F.-S. Yu *et al.*, *Discovery potentials of doubly charmed baryons*, Chin. Phys. **C42** (2018) 051001, [arXiv:1703.09086](#).
- [5] LHCb collaboration, A. A. Alves Jr. *et al.*, *The LHCb detector at the LHC*, JINST **3** (2008) S08005.
- [6] LHCb collaboration, R. Aaij *et al.*, *LHCb detector performance*, Int. J. Mod. Phys. **A30** (2015) 1530022, [arXiv:1412.6352](#).
- [7] R. Aaij *et al.*, *Performance of the LHCb Vertex Locator*, JINST **9** (2014) P09007, [arXiv:1405.7808](#).
- [8] R. Arink *et al.*, *Performance of the LHCb Outer Tracker*, JINST **9** (2014) P01002, [arXiv:1311.3893](#).
- [9] M. Adinolfi *et al.*, *Performance of the LHCb RICH detector at the LHC*, Eur. Phys. J. **C73** (2013) 2431, [arXiv:1211.6759](#).
- [10] A. A. Alves Jr. *et al.*, *Performance of the LHCb muon system*, JINST **8** (2013) P02022, [arXiv:1211.1346](#).
- [11] R. Aaij *et al.*, *The LHCb trigger and its performance in 2011*, JINST **8** (2013) P04022, [arXiv:1211.3055](#).
- [12] F. Archilli *et al.*, *Performance of the muon identification at LHCb*, JINST **8** (2013) P10020, [arXiv:1306.0249](#).
- [13] G. Dujany and B. Storaci, *Real-time alignment and calibration of the LHCb Detector in Run II*, J. Phys. Conf. Ser. **664** (2015) 082010.

- [14] T. Sjöstrand, S. Mrenna, and P. Skands, *A brief introduction to PYTHIA 8.1*, Comput. Phys. Commun. **178** (2008) 852, arXiv:0710.3820; T. Sjöstrand, S. Mrenna, and P. Skands, *PYTHIA 6.4 physics and manual*, JHEP **05** (2006) 026, arXiv:hep-ph/0603175.
- [15] I. Belyaev *et al.*, *Handling of the generation of primary events in Gauss, the LHCb simulation framework*, J. Phys. Conf. Ser. **331** (2011) 032047.
- [16] C.-H. Chang, J.-X. Wang, and X.-G. Wu, *GENXICC: a generator for hadronic production of the double heavy baryons Ξ_{cc} , Ξ_{bc} and Ξ_{bb}* , Comput. Phys. Commun. **177** (2007) 467, arXiv:hep-ph/0702054; C.-H. Chang, J.-X. Wang, and X.-G. Wu, *GENXICC2.0: an upgraded version of the generator for hadronic production of double heavy baryons Ξ_{cc} , Ξ_{bc} and Ξ_{bb}* , Comput. Phys. Commun. **181** (2010) 1144, arXiv:0910.4462.
- [17] D. J. Lange, *The EvtGen particle decay simulation package*, Nucl. Instrum. Meth. **A462** (2001) 152.
- [18] P. Golonka and Z. Was, *PHOTOS Monte Carlo: A precision tool for QED corrections in Z and W decays*, Eur. Phys. J. **C45** (2006) 97, arXiv:hep-ph/0506026.
- [19] Geant4 collaboration, J. Allison *et al.*, *Geant4 developments and applications*, IEEE Trans. Nucl. Sci. **53** (2006) 270; Geant4 collaboration, S. Agostinelli *et al.*, *Geant4: A simulation toolkit*, Nucl. Instrum. Meth. **A506** (2003) 250.
- [20] M. Clemencic *et al.*, *The LHCb simulation application, Gauss: Design, evolution and experience*, J. Phys. Conf. Ser. **331** (2011) 032023.
- [21] H. Voss, A. Hoecker, J. Stelzer, and F. Tegenfeldt, *TMVA - Toolkit for Multivariate Data Analysis*, PoS **ACAT** (2007) 040; A. Hoecker *et al.*, *TMVA 4 — Toolkit for Multivariate Data Analysis. Users Guide.*, arXiv:physics/0703039.
- [22] Particle Data Group, M. Tanabashi *et al.*, *Review of particle physics*, Phys. Rev. **D98** (2018) 030001.
- [23] W. D. Hulsbergen, *Decay chain fitting with a Kalman filter*, Nucl. Instrum. Meth. **A552** (2005) 566, arXiv:physics/0503191.
- [24] G. Punzi, *Sensitivity of searches for new signals and its optimization*, eConf **C030908** (2003) MODT002, arXiv:physics/0308063.
- [25] T. Skwarnicki, *A study of the radiative cascade transitions between the Upsilon-prime and Upsilon resonances*, PhD thesis, Institute of Nuclear Physics, Krakow, 1986, DESY-F31-86-02.
- [26] LHCb collaboration, R. Aaij *et al.*, *Measurement of the track reconstruction efficiency at LHCb*, JINST **10** (2015) P02007, arXiv:1408.1251.
- [27] LHCb collaboration, R. Aaij *et al.*, *Measurements of the branching fractions for $B_{(s)} \rightarrow D_{(s)}\pi\pi\pi$ and $\Lambda_b^0 \rightarrow \Lambda_c^+\pi\pi\pi$* , Phys. Rev. **D84** (2011) 092001, Erratum ibid. **D85** (2012) 039904, arXiv:1109.6831.

- [28] LHCb collaboration, R. Aaij *et al.*, *Measurement of b-hadron masses*, Phys. Lett. **B708** (2012) 241, [arXiv:1112.4896](https://arxiv.org/abs/1112.4896).
- [29] LHCb collaboration, R. Aaij *et al.*, *Precision measurement of D meson mass differences*, JHEP **06** (2013) 065, [arXiv:1304.6865](https://arxiv.org/abs/1304.6865).
- [30] L. Lyons, D. Gibaut, and P. Clifford, *How to combine correlated estimates of a single physical quantity*, Nucl. Instrum. Meth. **A270** (1988) 110.
- [31] A. Valassi, *Combining correlated measurements of several different physical quantities*, Nucl. Instrum. Meth. **A500** (2003) 391.
- [32] C. Alexandrou and C. Kallidonis, *Low-lying baryon masses using $N_f = 2$ twisted mass clover-improved fermions directly at the physical pion mass*, Phys. Rev. **D96** (2017) 034511, [arXiv:1704.02647](https://arxiv.org/abs/1704.02647).

LHCb collaboration

R. Aaij²⁷, B. Adeva⁴¹, M. Adinolfi⁴⁸, C.A. Aidala⁷³, Z. Ajaltouni⁵, S. Akar⁵⁹, P. Albicocco¹⁸, J. Albrecht¹⁰, F. Alessio⁴², M. Alexander⁵³, A. Alfonso Albero⁴⁰, S. Ali²⁷, G. Alkhazov³³, P. Alvarez Cartelle⁵⁵, A.A. Alves Jr⁴¹, S. Amato², S. Amerio²³, Y. Amhis⁷, L. An³, L. Anderlini¹⁷, G. Andreassi⁴³, M. Andreotti^{16,g}, J.E. Andrews⁶⁰, R.B. Appleby⁵⁶, F. Archilli²⁷, P. d'Argent¹², J. Arnau Romeu⁶, A. Artamonov³⁹, M. Artuso⁶¹, K. Arzymatov³⁷, E. Aslanides⁶, M. Atzeni⁴⁴, B. Audurier²², S. Bachmann¹², J.J. Back⁵⁰, S. Baker⁵⁵, V. Balagura^{7,b}, W. Baldini¹⁶, A. Baranov³⁷, R.J. Barlow⁵⁶, S. Barsuk⁷, W. Barter⁵⁶, F. Baryshnikov⁷⁰, V. Batozskaya³¹, B. Batsukh⁶¹, V. Battista⁴³, A. Bay⁴³, J. Beddow⁵³, F. Bedeschi²⁴, I. Bediaga¹, A. Beiter⁶¹, L.J. Bel²⁷, S. Belin²², N. Beliy⁶³, V. Bellee⁴³, N. Belloli^{20,i}, K. Belous³⁹, I. Belyaev^{34,42}, E. Ben-Haim⁸, G. Bencivenni¹⁸, S. Benson²⁷, S. Beranek⁹, A. Berezhnoy³⁵, R. Bernet⁴⁴, D. Berninghoff¹², E. Bertholet⁸, A. Bertolin²³, C. Betancourt⁴⁴, F. Betti^{15,42}, M.O. Bettler⁴⁹, M. van Beuzekom²⁷, Ia. Bezshyiko⁴⁴, S. Bhasin⁴⁸, J. Bhom²⁹, S. Bifani⁴⁷, P. Billoir⁸, A. Birnkraut¹⁰, A. Bizzeti^{17,u}, M. Bjørn⁵⁷, M.P. Blago⁴², T. Blake⁵⁰, F. Blanc⁴³, S. Blusk⁶¹, D. Bobulska⁵³, V. Bocci²⁶, O. Boente Garcia⁴¹, T. Boettcher⁵⁸, A. Bondar^{38,w}, N. Bondar³³, S. Borghi^{56,42}, M. Borisyak³⁷, M. Borsato⁴¹, F. Bossu⁷, M. Bouabdil⁹, T.J.V. Bowcock⁵⁴, C. Bozzi^{16,42}, S. Braun¹², M. Brodski⁴², J. Brodzicka²⁹, A. Brossa Gonzalo⁵⁰, D. Brundu²², E. Buchanan⁴⁸, A. Buonaura⁴⁴, C. Burr⁵⁶, A. Bursche²², J. Buytaert⁴², W. Byczynski⁴², S. Cadeddu²², H. Cai⁶⁴, R. Calabrese^{16,g}, R. Calladine⁴⁷, M. Calvi^{20,i}, M. Calvo Gomez^{40,m}, A. Camboni^{40,m}, P. Campana¹⁸, D.H. Campora Perez⁴², L. Capriotti⁵⁶, A. Carbone^{15,e}, G. Carboni²⁵, R. Cardinale^{19,h}, A. Cardini²², P. Carniti^{20,i}, L. Carson⁵², K. Carvalho Akiba², G. Casse⁵⁴, L. Cassina²⁰, M. Cattaneo⁴², G. Cavallero^{19,h}, R. Cenci^{24,p}, D. Chamont⁷, M.G. Chapman⁴⁸, M. Charles⁸, Ph. Charpentier⁴², G. Chatzikonstantinidis⁴⁷, M. Chefdeville⁴, V. Chekalina³⁷, C. Chen³, S. Chen²², S.-G. Chitic⁴², V. Chobanova⁴¹, M. Chrzaszcz⁴², A. Chubykin³³, P. Ciambrone¹⁸, X. Cid Vidal⁴¹, G. Ciezarek⁴², P.E.L. Clarke⁵², M. Clemencic⁴², H.V. Cliff⁴⁹, J. Closier⁴², V. Coco⁴², J.A.B. Coelho⁷, J. Cogan⁶, E. Cogneras⁵, L. Cojocariu³², P. Collins⁴², T. Colombo⁴², A. Comerma-Montells¹², A. Contu²², G. Coombs⁴², S. Coquereau⁴⁰, G. Corti⁴², M. Corvo^{16,g}, C.M. Costa Sobral⁵⁰, B. Couturier⁴², G.A. Cowan⁵², D.C. Craik⁵⁸, A. Crocombe⁵⁰, M. Cruz Torres¹, R. Currie⁵², C. D'Ambrosio⁴², F. Da Cunha Marinho², C.L. Da Silva⁷⁴, E. Dall'Occo²⁷, J. Dalseno⁴⁸, A. Danilina³⁴, A. Davis³, O. De Aguiar Francisco⁴², K. De Bruyn⁴², S. De Capua⁵⁶, M. De Cian⁴³, J.M. De Miranda¹, L. De Paula², M. De Serio^{14,d}, P. De Simone¹⁸, C.T. Dean⁵³, D. Decamp⁴, L. Del Buono⁸, B. Delaney⁴⁹, H.-P. Dembinski¹¹, M. Demmer¹⁰, A. Dendek³⁰, D. Derkach³⁷, O. Deschamps⁵, F. Desse⁷, F. Dettori⁵⁴, B. Dey⁶⁵, A. Di Canto⁴², P. Di Nezza¹⁸, S. Didenko⁷⁰, H. Dijkstra⁴², F. Dordei⁴², M. Dorigo^{42,y}, A. Dosil Suárez⁴¹, L. Douglas⁵³, A. Dovbnya⁴⁵, K. Dreimanis⁵⁴, L. Dufour²⁷, G. Dujany⁸, P. Durante⁴², J.M. Durham⁷⁴, D. Dutta⁵⁶, R. Dzhelyadin³⁹, M. Dziewiecki¹², A. Dziurda²⁹, A. Dzyuba³³, S. Easo⁵¹, U. Egede⁵⁵, V. Egorychev³⁴, S. Eidelman^{38,w}, S. Eisenhardt⁵², U. Eitschberger¹⁰, R. Ekelhof¹⁰, L. Eklund⁵³, S. Ely⁶¹, A. Ene³², S. Escher⁹, S. Esen²⁷, T. Evans⁵⁹, A. Falabella¹⁵, N. Farley⁴⁷, S. Farry⁵⁴, D. Fazzini^{20,42,i}, L. Federici²⁵, P. Fernandez Declara⁴², A. Fernandez Prieto⁴¹, F. Ferrari¹⁵, L. Ferreira Lopes⁴³, F. Ferreira Rodrigues², M. Ferro-Luzzi⁴², S. Filippov³⁶, R.A. Fini¹⁴, M. Fiorini^{16,g}, M. Firlej³⁰, C. Fitzpatrick⁴³, T. Fiutowski³⁰, F. Fleuret^{7,b}, M. Fontana^{22,42}, F. Fontanelli^{19,h}, R. Forty⁴², V. Franco Lima⁵⁴, M. Frank⁴², C. Frei⁴², J. Fu^{21,q}, W. Funk⁴², C. Färber⁴², M. Féo Pereira Rivello Carvalho²⁷, E. Gabriel⁵², A. Gallas Torreira⁴¹, D. Galli^{15,e}, S. Gallorini²³, S. Gambetta⁵², Y. Gan³, M. Gandelman², P. Gandini²¹, Y. Gao³, L.M. Garcia Martin⁷², B. Garcia Plana⁴¹, J. García Pardiñas⁴⁴, J. Garra Tico⁴⁹, L. Garrido⁴⁰, D. Gascon⁴⁰, C. Gaspar⁴², L. Gavard¹⁰, G. Gazzoni⁵, D. Gerick¹², E. Gersabeck⁵⁶, M. Gersabeck⁵⁶, T. Gershon⁵⁰, D. Gerstel⁶, Ph. Ghez⁴, S. Gianì⁴³, V. Gibson⁴⁹, O.G. Girard⁴³, L. Giubega³², K. Gizdov⁵², V.V. Gligorov⁸, D. Golubkov³⁴, A. Golutvin^{55,70}, A. Gomes^{1,a},

I.V. Gorelov³⁵, C. Gotti^{20,i}, E. Govorkova²⁷, J.P. Grabowski¹², R. Graciani Diaz⁴⁰,
 L.A. Granado Cardoso⁴², E. Graugés⁴⁰, E. Graverini⁴⁴, G. Graziani¹⁷, A. Grecu³², R. Greim²⁷,
 P. Griffith²², L. Grillo⁵⁶, L. Gruber⁴², B.R. Gruberg Cazon⁵⁷, O. Grünberg⁶⁷, C. Gu³,
 E. Gushchin³⁶, Yu. Guz^{39,42}, T. Gys⁴², C. Göbel⁶², T. Hadavizadeh⁵⁷, C. Hadjivasiliou⁵,
 G. Haefeli⁴³, C. Haen⁴², S.C. Haines⁴⁹, B. Hamilton⁶⁰, X. Han¹², T.H. Hancock⁵⁷,
 S. Hansmann-Menzemer¹², N. Harnew⁵⁷, S.T. Harnew⁴⁸, T. Harrison⁵⁴, C. Hasse⁴², M. Hatch⁴²,
 J. He⁶³, M. Hecker⁵⁵, K. Heinicke¹⁰, A. Heister¹⁰, K. Hennessy⁵⁴, L. Henry⁷²,
 E. van Herwijnen⁴², M. Heß⁶⁷, A. Hicheur², R. Hidalgo Charman⁵⁶, D. Hill⁵⁷, M. Hilton⁵⁶,
 P.H. Hopchev⁴³, W. Hu⁶⁵, W. Huang⁶³, Z.C. Huard⁵⁹, W. Hulsbergen²⁷, T. Humair⁵⁵,
 M. Hushchyn³⁷, D. Hutchcroft⁵⁴, D. Hynds²⁷, P. Ibis¹⁰, M. Idzik³⁰, P. Ilten⁴⁷, K. Ivshin³³,
 R. Jacobsson⁴², J. Jalocha⁵⁷, E. Jans²⁷, A. Jawahery⁶⁰, F. Jiang³, M. John⁵⁷, D. Johnson⁴²,
 C.R. Jones⁴⁹, C. Joram⁴², B. Jost⁴², N. Jurik⁵⁷, S. Kandybei⁴⁵, M. Karacson⁴², J.M. Kariuki⁴⁸,
 S. Karodia⁵³, N. Kazeev³⁷, M. Kecke¹², F. Keizer⁴⁹, M. Kelsey⁶¹, M. Kenzie⁴⁹, T. Ketel²⁸,
 E. Khairullin³⁷, B. Khanji¹², C. Khurewathanakul⁴³, K.E. Kim⁶¹, T. Kirn⁹, S. Klaver¹⁸,
 K. Klimaszewski³¹, T. Klimkovich¹¹, S. Koliiev⁴⁶, M. Kolpin¹², R. Kopecna¹², P. Koppenburg²⁷,
 I. Kostiuk²⁷, S. Kotriakhova³³, M. Kozeiha⁵, L. Kravchuk³⁶, M. Kreps⁵⁰, F. Kress⁵⁵,
 P. Krokovny^{38,w}, W. Krupa³⁰, W. Krzemien³¹, W. Kucewicz^{29,l}, M. Kucharczyk²⁹,
 V. Kudryavtsev^{38,w}, A.K. Kuonen⁴³, T. Kvaratskheliya^{34,42}, D. Lacarrere⁴², G. Lafferty⁵⁶,
 A. Lai²², D. Lancierini⁴⁴, G. Lanfranchi¹⁸, C. Langenbruch⁹, T. Latham⁵⁰, C. Lazzeroni⁴⁷,
 R. Le Gac⁶, A. Leflat³⁵, J. Lefrançois⁷, R. Lefèvre⁵, F. Lemaitre⁴², O. Leroy⁶, T. Lesiak²⁹,
 B. Leverington¹², P.-R. Li⁶³, T. Li³, Z. Li⁶¹, X. Liang⁶¹, T. Likhomanenko⁶⁹, R. Lindner⁴²,
 F. Lionetto⁴⁴, V. Lisovskyi⁷, X. Liu³, D. Loh⁵⁰, A. Loi²², I. Longstaff⁵³, J.H. Lopes²,
 G.H. Lovell⁴⁹, D. Lucchesi^{23,o}, M. Lucio Martinez⁴¹, A. Lupato²³, E. Luppi^{16,g}, O. Lupton⁴²,
 A. Lusiani²⁴, X. Lyu⁶³, F. Machefert⁷, F. Maciuc³², V. Macko⁴³, P. Mackowiak¹⁰,
 S. Maddrell-Mander⁴⁸, O. Maev^{33,42}, K. Maguire⁵⁶, D. Maisuzenko³³, M.W. Majewski³⁰,
 S. Malde⁵⁷, B. Malecki²⁹, A. Malinin⁶⁹, T. Maltsev^{38,w}, G. Manca^{22,f}, G. Mancinelli⁶,
 D. Marangotto^{21,q}, J. Maratas^{5,v}, J.F. Marchand⁴, U. Marconi¹⁵, C. Marin Benito⁷,
 M. Marinangeli⁴³, P. Marino⁴³, J. Marks¹², P.J. Marshall⁵⁴, G. Martellotti²⁶, M. Martin⁶,
 M. Martinelli⁴², D. Martinez Santos⁴¹, F. Martinez Vidal⁷², A. Massafferri¹, M. Materok⁹,
 R. Matev⁴², A. Mathad⁵⁰, Z. Mathe⁴², C. Matteuzzi²⁰, A. Mauri⁴⁴, E. Maurice^{7,b}, B. Maurin⁴³,
 A. Mazurov⁴⁷, M. McCann^{55,42}, A. McNab⁵⁶, R. McNulty¹³, J.V. Mead⁵⁴, B. Meadows⁵⁹,
 C. Meaux⁶, F. Meier¹⁰, N. Meinert⁶⁷, D. Melnychuk³¹, M. Merk²⁷, A. Merli^{21,q}, E. Michielin²³,
 D.A. Milanes⁶⁶, E. Millard⁵⁰, M.-N. Minard⁴, L. Minzoni^{16,g}, D.S. Mitzel¹², A. Mogini⁸,
 J. Molina Rodriguez^{1,z}, T. Mombächer¹⁰, I.A. Monroy⁶⁶, S. Monteil⁵, M. Morandin²³,
 G. Morello¹⁸, M.J. Morello^{24,t}, O. Morgunova⁶⁹, J. Moron³⁰, A.B. Morris⁶, R. Mountain⁶¹,
 F. Muheim⁵², M. Mulder²⁷, C.H. Murphy⁵⁷, D. Murray⁵⁶, A. Mödden¹⁰, D. Müller⁴²,
 J. Müller¹⁰, K. Müller⁴⁴, V. Müller¹⁰, P. Naik⁴⁸, T. Nakada⁴³, R. Nandakumar⁵¹, A. Nandi⁵⁷,
 T. Nanut⁴³, I. Nasteva², M. Needham⁵², N. Neri²¹, S. Neubert¹², N. Neufeld⁴², M. Neuner¹²,
 T.D. Nguyen⁴³, C. Nguyen-Mau^{43,n}, S. Nieswand⁹, R. Niet¹⁰, N. Nikitin³⁵, A. Nogay⁶⁹,
 N.S. Nolte⁴², D.P. O'Hanlon¹⁵, A. Oblakowska-Mucha³⁰, V. Obraztsov³⁹, S. Ogilvy¹⁸,
 R. Oldeman^{22,f}, C.J.G. Onderwater⁶⁸, A. Ossowska²⁹, J.M. Otalora Goicochea², P. Owen⁴⁴,
 A. Oyanguren⁷², P.R. Pais⁴³, T. Pajero^{24,t}, A. Palano¹⁴, M. Palutan^{18,42}, G. Pashkin⁷¹,
 A. Papanestis⁵¹, M. Pappagallo⁵², L.L. Pappalardo^{16,g}, W. Parker⁶⁰, C. Parkes⁵⁶,
 G. Passaleva^{17,42}, A. Pastore¹⁴, M. Patel⁵⁵, C. Patrignani^{15,e}, A. Pearce⁴², A. Pellegrino²⁷,
 G. Penso²⁶, M. Pepe Altarelli⁴², S. Perazzini⁴², D. Pereima³⁴, P. Perret⁵, L. Pescatore⁴³,
 K. Petridis⁴⁸, A. Petrolini^{19,h}, A. Petrov⁶⁹, S. Petrucci⁵², M. Petruzzo^{21,q}, B. Pietrzyk⁴,
 G. Pietrzyk⁴³, M. Pikies²⁹, M. Pili⁵⁷, D. Pinci²⁶, J. Pinzino⁴², F. Pisani⁴², A. Piucci¹²,
 V. Placinta³², S. Playfer⁵², J. Plews⁴⁷, M. Plo Casasus⁴¹, F. Polci⁸, M. Poli Lener¹⁸,
 A. Poluektov⁵⁰, N. Polukhina^{70,c}, I. Polyakov⁶¹, E. Polycarpo², G.J. Pomery⁴⁸, S. Ponce⁴²,
 A. Popov³⁹, D. Popov^{47,11}, S. Poslavskii³⁹, C. Potterat², E. Price⁴⁸, J. Prisciandaro⁴¹,

C. Prouve⁴⁸, V. Pugatch⁴⁶, A. Puig Navarro⁴⁴, H. Pullen⁵⁷, G. Punzi^{24,p}, W. Qian⁶³, J. Qin⁶³, R. Quagliani⁸, B. Quintana⁵, B. Rachwal³⁰, J.H. Rademacker⁴⁸, M. Rama²⁴, M. Ramos Pernas⁴¹, M.S. Rangel², F. Ratnikov^{37,x}, G. Raven²⁸, M. Ravonel Salzgeber⁴², M. Reboud⁴, F. Redi⁴³, S. Reichert¹⁰, A.C. dos Reis¹, F. Reiss⁸, C. Remon Alepuz⁷², Z. Ren³, V. Renaudin⁷, S. Ricciardi⁵¹, S. Richards⁴⁸, K. Rinnert⁵⁴, P. Robbe⁷, A. Robert⁸, A.B. Rodrigues⁴³, E. Rodrigues⁵⁹, J.A. Rodriguez Lopez⁶⁶, M. Roehrken⁴², A. Rogozhnikov³⁷, S. Roiser⁴², A. Rollings⁵⁷, V. Romanovskiy³⁹, A. Romero Vidal⁴¹, M. Rotondo¹⁸, M.S. Rudolph⁶¹, T. Ruf⁴², J. Ruiz Vidal⁷², J.J. Saborido Silva⁴¹, N. Sagidova³³, B. Saitta^{22,f}, V. Salustino Guimaraes⁶², C. Sanchez Gras²⁷, C. Sanchez Mayordomo⁷², B. Sanmartin Sedes⁴¹, R. Santacesaria²⁶, C. Santamarina Rios⁴¹, M. Santimaria¹⁸, E. Santovetti^{25,j}, G. Sarpis⁵⁶, A. Sarti^{18,k}, C. Satriano^{26,s}, A. Satta²⁵, M. Saur⁶³, D. Savrina^{34,35}, S. Schael⁹, M. Schellenberg¹⁰, M. Schiller⁵³, H. Schindler⁴², M. Schmelling¹¹, T. Schmelzer¹⁰, B. Schmidt⁴², O. Schneider⁴³, A. Schopper⁴², H.F. Schreiner⁵⁹, M. Schubiger⁴³, M.H. Schune⁷, R. Schwemmer⁴², B. Sciascia¹⁸, A. Sciubba^{26,k}, A. Semennikov³⁴, E.S. Sepulveda⁸, A. Sergi^{47,42}, N. Serra⁴⁴, J. Serrano⁶, L. Sestini²³, A. Seuthe¹⁰, P. Seyfert⁴², M. Shapkin³⁹, Y. Shcheglov^{33,†}, T. Shears⁵⁴, L. Shekhtman^{38,w}, V. Shevchenko⁶⁹, E. Shmanin⁷⁰, B.G. Siddi¹⁶, R. Silva Coutinho⁴⁴, L. Silva de Oliveira², G. Simi^{23,o}, S. Simone^{14,d}, N. Skidmore¹², T. Skwarnicki⁶¹, J.G. Smeaton⁴⁹, E. Smith⁹, I.T. Smith⁵², M. Smith⁵⁵, M. Soares¹⁵, I. Soares Lavra¹, M.D. Sokoloff⁵⁹, F.J.P. Soler⁵³, B. Souza De Paula², B. Spaan¹⁰, P. Spradlin⁵³, F. Stagni⁴², M. Stahl¹², S. Stahl⁴², P. Steffko⁴³, S. Stefkova⁵⁵, O. Steinkamp⁴⁴, S. Stemmle¹², O. Stenyakin³⁹, M. Stepanova³³, H. Stevens¹⁰, A. Stocchi⁷, S. Stone⁶¹, B. Storaci⁴⁴, S. Stracka^{24,p}, M.E. Stramaglia⁴³, M. Stratificiuc³², U. Straumann⁴⁴, S. Strokov⁷¹, J. Sun³, L. Sun⁶⁴, K. Swientek³⁰, V. Syropoulos²⁸, T. Szumlak³⁰, M. Szymanski⁶³, S. T'Jampens⁴, Z. Tang³, A. Tayduganov⁶, T. Tekampe¹⁰, G. Tellarini¹⁶, F. Teubert⁴², E. Thomas⁴², J. van Tilburg²⁷, M.J. Tilley⁵⁵, V. Tisserand⁵, M. Tobin³⁰, S. Tolk⁴², L. Tomassetti^{16,g}, D. Tonelli²⁴, D.Y. Tou⁸, R. Tourinho Jadallah Aoude¹, E. Tournefier⁴, M. Traill⁵³, M.T. Tran⁴³, A. Trisovic⁴⁹, A. Tsaregorodtsev⁶, G. Tuci²⁴, A. Tully⁴⁹, N. Tuning^{27,42}, A. Ukleja³¹, A. Usachov⁷, A. Ustyuzhanin³⁷, U. Uwer¹², A. Vagner⁷¹, V. Vagnoni¹⁵, A. Valassi⁴², S. Valat⁴², G. Valenti¹⁵, R. Vazquez Gomez⁴², P. Vazquez Regueiro⁴¹, S. Vecchi¹⁶, M. van Veghel²⁷, J.J. Velthuis⁴⁸, M. Veltri^{17,r}, G. Veneziano⁵⁷, A. Venkateswaran⁶¹, T.A. Verlage⁹, M. Vernet⁵, M. Veronesi²⁷, N.V. Veronika¹³, M. Vesterinen⁵⁷, J.V. Viana Barbosa⁴², D. Vieira⁶³, M. Vieites Diaz⁴¹, H. Viemann⁶⁷, X. Vilasis-Cardona^{40,m}, A. Vitkovskiy²⁷, M. Vitti⁴⁹, V. Volkov³⁵, A. Vollhardt⁴⁴, B. Voneki⁴², A. Vorobyev³³, V. Vorobyev^{38,w}, J.A. de Vries²⁷, C. Vázquez Sierra²⁷, R. Waldi⁶⁷, J. Walsh²⁴, J. Wang⁶¹, M. Wang³, Y. Wang⁶⁵, Z. Wang⁴⁴, D.R. Ward⁴⁹, H.M. Wark⁵⁴, N.K. Watson⁴⁷, D. Websdale⁵⁵, A. Weiden⁴⁴, C. Weisser⁵⁸, M. Whitehead⁹, J. Wicht⁵⁰, G. Wilkinson⁵⁷, M. Wilkinson⁶¹, I. Williams⁴⁹, M.R.J. Williams⁵⁶, M. Williams⁵⁸, T. Williams⁴⁷, F.F. Wilson^{51,42}, J. Wimberley⁶⁰, M. Winn⁷, J. Wishahi¹⁰, W. Wislicki³¹, M. Witek²⁹, G. Wormser⁷, S.A. Wotton⁴⁹, K. Wyllie⁴², D. Xiao⁶⁵, Y. Xie⁶⁵, A. Xu³, M. Xu⁶⁵, Q. Xu⁶³, Z. Xu³, Z. Xu⁴, Z. Yang³, Z. Yang⁶⁰, Y. Yao⁶¹, L.E. Yeomans⁵⁴, H. Yin⁶⁵, J. Yu^{65,ab}, X. Yuan⁶¹, O. Yushchenko³⁹, K.A. Zarebski⁴⁷, M. Zavertyaev^{11,c}, D. Zhang⁶⁵, L. Zhang³, W.C. Zhang^{3,aa}, Y. Zhang⁷, A. Zhelezov¹², Y. Zheng⁶³, X. Zhu³, V. Zhukov^{9,35}, J.B. Zonneveld⁵², S. Zucchelli¹⁵.

¹Centro Brasileiro de Pesquisas Físicas (CBPF), Rio de Janeiro, Brazil

²Universidade Federal do Rio de Janeiro (UFRJ), Rio de Janeiro, Brazil

³Center for High Energy Physics, Tsinghua University, Beijing, China

⁴Univ. Grenoble Alpes, Univ. Savoie Mont Blanc, CNRS, IN2P3-LAPP, Annecy, France

⁵Clermont Université, Université Blaise Pascal, CNRS/IN2P3, LPC, Clermont-Ferrand, France

⁶Aix Marseille Univ, CNRS/IN2P3, CPPM, Marseille, France

⁷LAL, Univ. Paris-Sud, CNRS/IN2P3, Université Paris-Saclay, Orsay, France

⁸LPNHE, Sorbonne Université, Paris Diderot Sorbonne Paris Cité, CNRS/IN2P3, Paris, France

- ⁹*I. Physikalisches Institut, RWTH Aachen University, Aachen, Germany*
- ¹⁰*Fakultät Physik, Technische Universität Dortmund, Dortmund, Germany*
- ¹¹*Max-Planck-Institut für Kernphysik (MPIK), Heidelberg, Germany*
- ¹²*Physikalisches Institut, Ruprecht-Karls-Universität Heidelberg, Heidelberg, Germany*
- ¹³*School of Physics, University College Dublin, Dublin, Ireland*
- ¹⁴*INFN Sezione di Bari, Bari, Italy*
- ¹⁵*INFN Sezione di Bologna, Bologna, Italy*
- ¹⁶*INFN Sezione di Ferrara, Ferrara, Italy*
- ¹⁷*INFN Sezione di Firenze, Firenze, Italy*
- ¹⁸*INFN Laboratori Nazionali di Frascati, Frascati, Italy*
- ¹⁹*INFN Sezione di Genova, Genova, Italy*
- ²⁰*INFN Sezione di Milano-Bicocca, Milano, Italy*
- ²¹*INFN Sezione di Milano, Milano, Italy*
- ²²*INFN Sezione di Cagliari, Monserrato, Italy*
- ²³*INFN Sezione di Padova, Padova, Italy*
- ²⁴*INFN Sezione di Pisa, Pisa, Italy*
- ²⁵*INFN Sezione di Roma Tor Vergata, Roma, Italy*
- ²⁶*INFN Sezione di Roma La Sapienza, Roma, Italy*
- ²⁷*Nikhef National Institute for Subatomic Physics, Amsterdam, Netherlands*
- ²⁸*Nikhef National Institute for Subatomic Physics and VU University Amsterdam, Amsterdam, Netherlands*
- ²⁹*Henryk Niewodniczanski Institute of Nuclear Physics Polish Academy of Sciences, Kraków, Poland*
- ³⁰*AGH - University of Science and Technology, Faculty of Physics and Applied Computer Science, Kraków, Poland*
- ³¹*National Center for Nuclear Research (NCBJ), Warsaw, Poland*
- ³²*Horia Hulubei National Institute of Physics and Nuclear Engineering, Bucharest-Magurele, Romania*
- ³³*Petersburg Nuclear Physics Institute (PNPI), Gatchina, Russia*
- ³⁴*Institute of Theoretical and Experimental Physics (ITEP), Moscow, Russia*
- ³⁵*Institute of Nuclear Physics, Moscow State University (SINP MSU), Moscow, Russia*
- ³⁶*Institute for Nuclear Research of the Russian Academy of Sciences (INR RAS), Moscow, Russia*
- ³⁷*Yandex School of Data Analysis, Moscow, Russia*
- ³⁸*Budker Institute of Nuclear Physics (SB RAS), Novosibirsk, Russia*
- ³⁹*Institute for High Energy Physics (IHEP), Protvino, Russia*
- ⁴⁰*ICCUB, Universitat de Barcelona, Barcelona, Spain*
- ⁴¹*Instituto Galego de Física de Altas Enerxías (IGFAE), Universidade de Santiago de Compostela, Santiago de Compostela, Spain*
- ⁴²*European Organization for Nuclear Research (CERN), Geneva, Switzerland*
- ⁴³*Institute of Physics, Ecole Polytechnique Fédérale de Lausanne (EPFL), Lausanne, Switzerland*
- ⁴⁴*Physik-Institut, Universität Zürich, Zürich, Switzerland*
- ⁴⁵*NSC Kharkiv Institute of Physics and Technology (NSC KIPT), Kharkiv, Ukraine*
- ⁴⁶*Institute for Nuclear Research of the National Academy of Sciences (KINR), Kyiv, Ukraine*
- ⁴⁷*University of Birmingham, Birmingham, United Kingdom*
- ⁴⁸*H.H. Wills Physics Laboratory, University of Bristol, Bristol, United Kingdom*
- ⁴⁹*Cavendish Laboratory, University of Cambridge, Cambridge, United Kingdom*
- ⁵⁰*Department of Physics, University of Warwick, Coventry, United Kingdom*
- ⁵¹*STFC Rutherford Appleton Laboratory, Didcot, United Kingdom*
- ⁵²*School of Physics and Astronomy, University of Edinburgh, Edinburgh, United Kingdom*
- ⁵³*School of Physics and Astronomy, University of Glasgow, Glasgow, United Kingdom*
- ⁵⁴*Oliver Lodge Laboratory, University of Liverpool, Liverpool, United Kingdom*
- ⁵⁵*Imperial College London, London, United Kingdom*
- ⁵⁶*School of Physics and Astronomy, University of Manchester, Manchester, United Kingdom*
- ⁵⁷*Department of Physics, University of Oxford, Oxford, United Kingdom*
- ⁵⁸*Massachusetts Institute of Technology, Cambridge, MA, United States*
- ⁵⁹*University of Cincinnati, Cincinnati, OH, United States*
- ⁶⁰*University of Maryland, College Park, MD, United States*
- ⁶¹*Syracuse University, Syracuse, NY, United States*

- ⁶²*Pontifícia Universidade Católica do Rio de Janeiro (PUC-Rio), Rio de Janeiro, Brazil, associated to* ²
- ⁶³*University of Chinese Academy of Sciences, Beijing, China, associated to* ³
- ⁶⁴*School of Physics and Technology, Wuhan University, Wuhan, China, associated to* ³
- ⁶⁵*Institute of Particle Physics, Central China Normal University, Wuhan, Hubei, China, associated to* ³
- ⁶⁶*Departamento de Física , Universidad Nacional de Colombia, Bogota, Colombia, associated to* ⁸
- ⁶⁷*Institut für Physik, Universität Rostock, Rostock, Germany, associated to* ¹²
- ⁶⁸*Van Swinderen Institute, University of Groningen, Groningen, Netherlands, associated to* ²⁷
- ⁶⁹*National Research Centre Kurchatov Institute, Moscow, Russia, associated to* ³⁴
- ⁷⁰*National University of Science and Technology "MISIS", Moscow, Russia, associated to* ³⁴
- ⁷¹*National Research Tomsk Polytechnic University, Tomsk, Russia, associated to* ³⁴
- ⁷²*Instituto de Física Corpuscular, Centro Mixto Universidad de Valencia - CSIC, Valencia, Spain, associated to* ⁴⁰
- ⁷³*University of Michigan, Ann Arbor, United States, associated to* ⁶¹
- ⁷⁴*Los Alamos National Laboratory (LANL), Los Alamos, United States, associated to* ⁶¹

^a*Universidade Federal do Triângulo Mineiro (UFTM), Uberaba-MG, Brazil*

^b*Laboratoire Leprince-Ringuet, Palaiseau, France*

^c*P.N. Lebedev Physical Institute, Russian Academy of Science (LPI RAS), Moscow, Russia*

^d*Università di Bari, Bari, Italy*

^e*Università di Bologna, Bologna, Italy*

^f*Università di Cagliari, Cagliari, Italy*

^g*Università di Ferrara, Ferrara, Italy*

^h*Università di Genova, Genova, Italy*

ⁱ*Università di Milano Bicocca, Milano, Italy*

^j*Università di Roma Tor Vergata, Roma, Italy*

^k*Università di Roma La Sapienza, Roma, Italy*

^l*AGH - University of Science and Technology, Faculty of Computer Science, Electronics and Telecommunications, Kraków, Poland*

^m*LIFAELS, La Salle, Universitat Ramon Llull, Barcelona, Spain*

ⁿ*Hanoi University of Science, Hanoi, Vietnam*

^o*Università di Padova, Padova, Italy*

^p*Università di Pisa, Pisa, Italy*

^q*Università degli Studi di Milano, Milano, Italy*

^r*Università di Urbino, Urbino, Italy*

^s*Università della Basilicata, Potenza, Italy*

^t*Scuola Normale Superiore, Pisa, Italy*

^u*Università di Modena e Reggio Emilia, Modena, Italy*

^v*MSU - Iligan Institute of Technology (MSU-IIT), Iligan, Philippines*

^w*Novosibirsk State University, Novosibirsk, Russia*

^x*National Research University Higher School of Economics, Moscow, Russia*

^y*Sezione INFN di Trieste, Trieste, Italy*

^z*Escuela Agrícola Panamericana, San Antonio de Oriente, Honduras*

^{aa}*School of Physics and Information Technology, Shaanxi Normal University (SNNU), Xi'an, China*

^{ab}*Physics and Micro Electronic College, Hunan University, Changsha City, China*

[†]*Deceased*

1 Supplementary material for LHCb-PAPER-2018-026

Figure 3 shows the comparison between Ξ_{cc}^{++} mass measured from $\Xi_{cc}^{++} \rightarrow \Lambda_c^+ K^- \pi^+ \pi^+$ and $\Xi_{cc}^{++} \rightarrow \Xi_c^+ \pi^+$ channel, and the combined mass value using these two results.

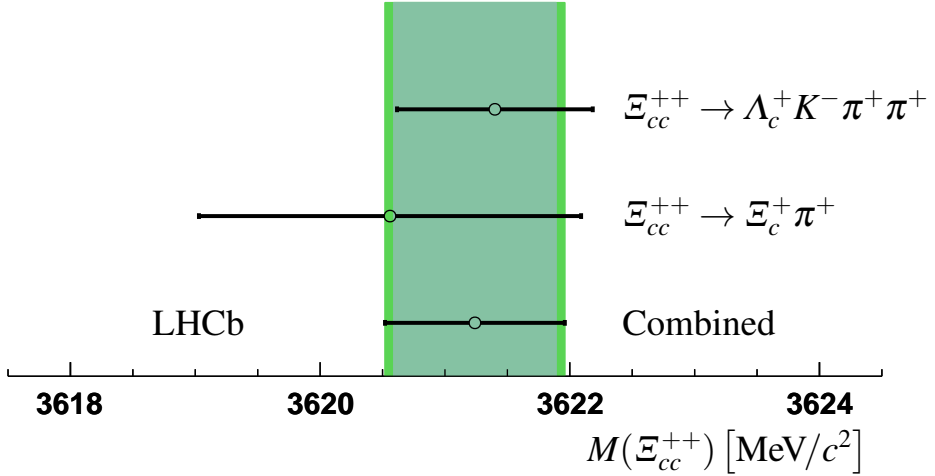


Figure 3: Measured Ξ_{cc}^{++} masses obtained with the decay modes $\Xi_{cc}^{++} \rightarrow \Lambda_c^+ K^- \pi^+ \pi^+$ and $\Xi_{cc}^{++} \rightarrow \Xi_c^+ \pi^+$, and the combined result. The darker green band represents the statistical uncertainty on the combination, and the lighter green band represents the total uncertainty on the combination.